



Strain Monitoring in Stiffened Composite Panels Using Embedded Fibre Optical and Strain Gauge Sensors

Roman Růžek, Martin Kadlec, Konstantinos Tserpes, Evangelos Karachalios

► To cite this version:

Roman Růžek, Martin Kadlec, Konstantinos Tserpes, Evangelos Karachalios. Strain Monitoring in Stiffened Composite Panels Using Embedded Fibre Optical and Strain Gauge Sensors. EWSHM - 7th European Workshop on Structural Health Monitoring, IFFSTTAR, Inria, Université de Nantes, Jul 2014, Nantes, France. hal-01022004

HAL Id: hal-01022004

<https://inria.hal.science/hal-01022004>

Submitted on 10 Jul 2014

HAL is a multi-disciplinary open access archive for the deposit and dissemination of scientific research documents, whether they are published or not. The documents may come from teaching and research institutions in France or abroad, or from public or private research centers.

L'archive ouverte pluridisciplinaire **HAL**, est destinée au dépôt et à la diffusion de documents scientifiques de niveau recherche, publiés ou non, émanant des établissements d'enseignement et de recherche français ou étrangers, des laboratoires publics ou privés.

STRAIN MONITORING IN STIFFENED COMPOSITE PANELS USING EMBEDDED FIBRE OPTICAL AND STRAIN GAUGE SENSORS

Roman Růžek¹, Martin Kadlec¹, Konstantinos Tserpes², Evangelos Karachalios³

¹ *Výzkumný a zkušební letecký ústav, a.s. (VZLÚ), Beranových 130, 199 05 Prague 9 - Letnany, Czech Republic*

² *Laboratory of Technology & Strength of Materials, Department of Mechanical Engineering & Aeronautics, University of Patras, Patras 26500, Greece*

³ *Hellenic Aerospace Industry, Research and Development Department, 320 09 Schimatari, Greece*

ruzek@vzlu.cz

ABSTRACT

This paper describes an implemented structural health monitoring (SHM) system based on Fibre Optic Bragg Grating (FOBG) sensors and standard resistance strain gauges (SGs) placed onto/into a stiffened carbon fibre-reinforced polymer (CFRP) fuselage panel. The role of the FOBG sensor system was to monitor the structural integrity of the reference, impacted and fatigued panels under compression loading. The FOBG and/or SG sensors were placed (embedded or bonded) at various locations into and/or onto the structure. The functionality of the SHM system was verified by experimental evaluation. The comparability and reliability of the results gained from the FOBG sensors and resistance strain gauges is discussed. This paper presents the key objectives from a European Union funded collaborative Project, inside the Clean Sky Joint Technology Initiative (CS JTI), investigating the SHM systems for CFRP fuselage stiffened panels based on fibre optic Bragg grating sensors for the Green Regional Aircraft Integrated Technology Demonstrator (GRA ITD)

KEYWORDS: *composite, stiffened panel, sensors, optical fibre, strain gauge.*

INTRODUCTION

The service lifetime of a structure depends on the ability to detect and monitor potentially developing of defects, operational damages and crack initiation and propagation, among other things. Structural health monitoring (SHM) is one of the most rapidly developing fields of interest considering the service lifetime. There are a variety of available approaches for SHM. Among these approaches, methods based on optical [1]-[6] sensors are among the most rapidly developing methods.

This paper is focused on the use of Fibre Optic Bragg Grating (FOBG) strain sensors for aerospace applications. FOBG sensors were applied into and/or onto a carbon fibre-reinforced composite panel (CFRP). A comparison of the FOBG results with the standard resistance strain gauges data is one of paper objectives. FOBG sensors can be interrogated with different types of opto-electronic instrumentation. The equipment and sensors used for the stiffened panel behaviour assessment are described in the paper. The capability of FOBG for the strain monitoring of composite structures was discussed in the past. The paper is focused on the potential problems involved in the interpretation of the results based on sensors embedded into the structure due to the local stability lost. The functionality of the SHM system was verified by experimental evaluation of three fuselage panels. Experimental evaluation was conducted by means of static and fatigue compression loading. The fibre sensors were embedded into the panel so as to minimise risk of fibre breakage during manufacturing and impact testing and also to effectively capture strains that are representative of the damage developed in the panel due to compressive load.

1 PANEL AND TEST METHODOLOGY DESCRIPTION

Three stiffened composite panels were used for evaluation of the behaviour of the sensors. The panels consist of the skin and three omega stringers. Each panel was made from the unidirectional HexPly 8552 (by Hexcel) prepreg composite material, which is a high performance tough epoxy matrix prepreg that is used in primary aerospace structures. The composite material exhibits good impact resistance and damage tolerance for a wide range of applications. The layup of the skin was $[45^\circ/90^\circ/-45^\circ/0^\circ/45^\circ/90^\circ/-45^\circ/0^\circ]_s$ and that of the stringers was $[45^\circ/-45^\circ/0^\circ_2/90^\circ/0^\circ]_s$.

With the scope of the development and verification of the SHM system based on FOBGs, the following loading scenarios were chosen:

- Compression to failure of an undamaged panel (Panel_1);
- Compression to failure of a panel with barely visible impact damage (BVID) after fatigue (Panel_2);
- Compression to failure of a panel with visible impact damage (VID) (Panel_3).

The specific loading conditions were chosen because they are highly representative for a bottom fuselage panel. Moreover, compression after impact is generally the most representative test for composite panels. The BVID and VID locations were determined so as to influence the performance of the overall panel. The external dimensions of the panel were 1650×900 mm. Each of the panels in this study contains aluminium blocks at each end to enable the introduction of accurate compressive load. A special anti-buckling frame was designed and manufactured with the aim of achieving test boundary conditions that are very similar to those in real application. The static and fatigue tests were conducted using a 1 MN MTS hydraulic frame with a TestFlex®40 control system [7]. The test arrangement of the panel in the MTS hydraulic test stand is shown in Figure 1.

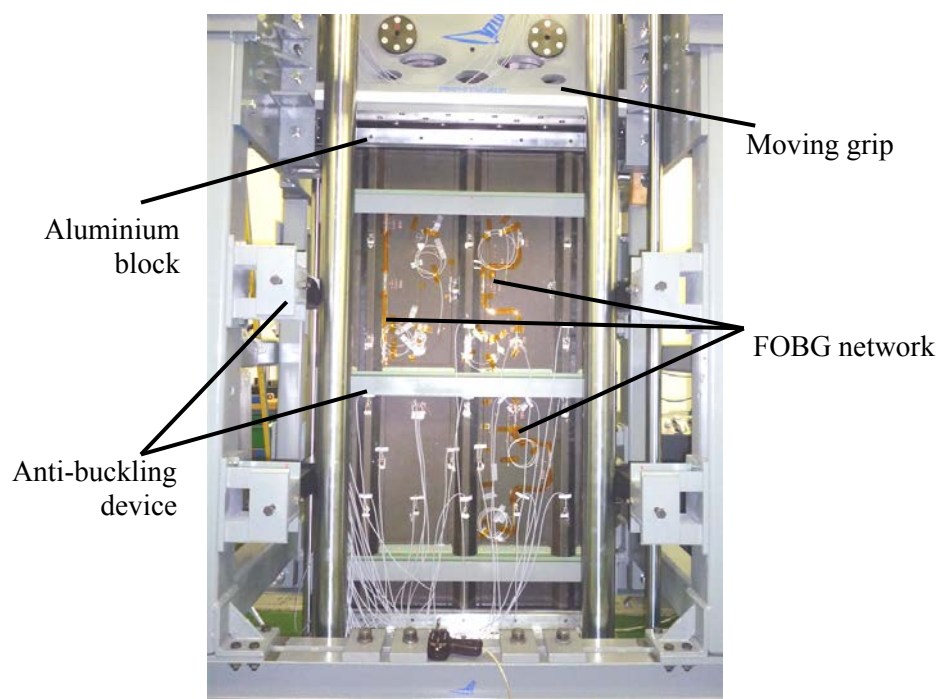


Figure 1: Panel compression test configuration in the 1 MN MTS stand

2 DESCRIPTION OF THE FOBG AND STRAIN GAUGES

The network of FOBG sensors was designed to enable measurement of the strains that are related to the basic damage patterns developed in the panel during loading. Two main failure modes were expected: buckling in the bay and buckling of the stringers. Sensors located in the bay area can

effectively monitor buckling initiation and the alteration of buckling modes. Sensors placed at the stringers can monitor the buckling initiation that causes failure of the panel.

At each of the three panels, nine FOBGs were mounted (Figures 1, 2, and 3) following a configuration of three sensors per line. The position of the sensors in the network in the panel is shown in Figure 3. The optical sensors were placed in the middle section of the bays as well as at the edge of the stringers foot. In Panel_1, the sensors were bonded externally. The sensors were bonded by cyanoacrylate adhesive onto the selected positions on the panel. Next, a slightly larger length of the fibre optic (including the FOBG) was covered with standard two part epoxy paste adhesive (Araldite® 2015 by HUNTSMAN) for extra protection and bonding security. In Panel_2 and Panel_3, the sensors were embedded into the structure. Embedment of the FOBG sensors during manufacturing is a tedious task because it involves many difficulties, such as the selection of ingress and egress points of the sensor data lines, the possible effect of the embedded sensors and ancillaries on the mechanical properties of the composite and the risk of sensor breakage during fabrication. The FiberSensing FOBG sensors were used in the arrays of three sensors. The wavelengths of the sensors at each array for Panel_1, Panel_2, and Panel_3 were 1526 nm, 1547 nm, and 1568 nm, respectively. Due to the intense temperature/pressure conditions occurring during curing, the primary coating of the optical fibre was polyimide with a polyimide recoating on the grating location after inscription of the FOBGs to improve the mechanical performance. The FOBG lines were embedded “bare” (without any buffer protection) so that there is direct strain transfer from the laminate to the FOBGs. Only at the position of ingress/egress points was placed a small length of buffer cable (typ. 0.4 mm in diameter - also polyimide) for extra protection of the fibre. FC/APC connectors were placed on the fibre optic cables using the standard splicing process. Figure 2 shows an example of embedded FOBG routing in a panel with the egress and ingress point definition.

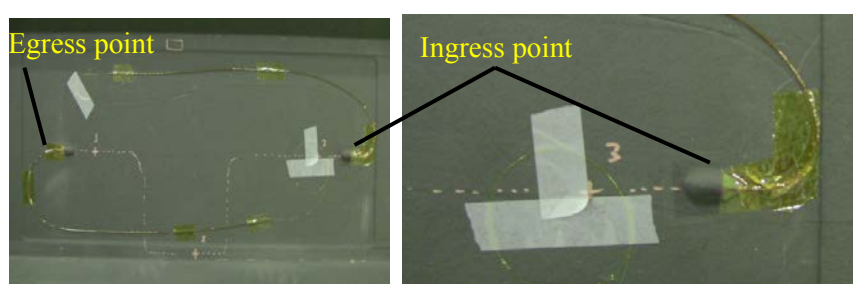


Figure 2: Embedded FOBGs routing on damaged BVID / manufacturing defects configuration (Panel_2)

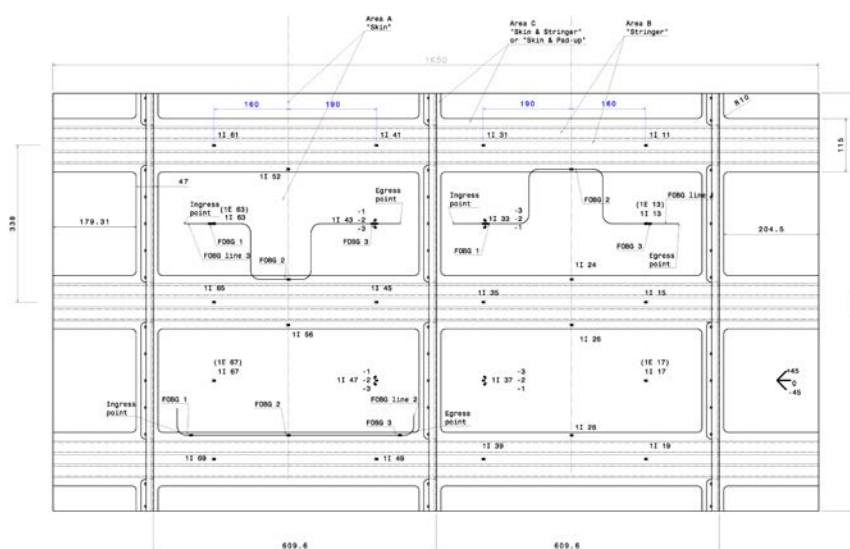


Figure 3: Definition of the locations of the strain gauges and the FOBG sensors (Panel_1)

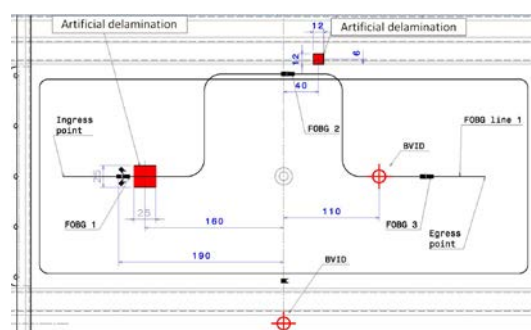


Figure 4: Definition of the locations of the FOBG sensors in line 1 of Panel_2

In Panel_1 and Panel_2, the sensors were placed at the bays of the same side with respect to the axis of the panel, while in Panel_3, the sensors were placed at anti-symmetric bays. In Panel_2, the sensors placed at the middle of the bays are very close to the artificial delamination as well as to the impact damage sites (Figure 4). Thus, they are expected to capture any phenomena developed there, due to the concentration of the initial damage, by recording the extreme values of strain. In general, the three lines of the FOBG sensors were mounted into the panels –line 1 and line 3 each contain two sensors on the bay (L1S1, L1S3, L3S1, L3S3) and one sensor on the stringer foot (L1S2, L3S2); line 2 contains three sensors on the stringer foot (L2S1, L2S2, L2S3).

To be able to validate the measurements given by the FOBGs, a large number of linear and rosette resistance strain gauges were mounted externally to the panels. 69 strain gauges channels were measured for each panel. The strain gauges were placed at different positions on the bays and omega stringers (at the foot and the top of stringers), as shown in Figure 3 and Figure 4.

Data from the strain gauges were recorded, stored and evaluated using a BMC Messsysteme GmbH equipment [8]. The system was controlled using the NextView 4.2 data acquisition software [9]. The FBGuard (Safibra producer) 4-channel high accuracy FOBG static and dynamic measuring device [10] with the following parameters for strain measurement was used:

- Main wavelength bulk is set at $1550 \text{ nm} \pm 20 \text{ nm}$;
- Wavelength accuracy is $\leq 15 \text{ pm}$, and the wavelength resolution is $\leq 1 \text{ pm}$;
- Scan frequency (sampling) up to 300 Hz;
- Minimum channel switching delay time 10 ms; optical connector FC/APC;
- Dynamic range 20 dB; laser class (IEC 60825-1) 1.



Figure 5: FOBG FBGuard measuring device and evaluation PC with FBGuard web interface

Data acquisition was performed by an embedded device PC and data transfer was accomplished via the SSH protocol(s). The system was used to evaluate the wavelength-intensity FOBG sensor peak position via the centre of gravity method and computes strain from the peak position using the known sensor length (alternatively, Gaussian approximation was available to determine the peak position, but for this purpose it was not required). The scan frequency was set to the maximum rate (300 Hz), the channel switching frequency was set to 1 Hz, and the averaging interval was set to 1 s. Therefore, it was certain that from each 3-second period of a measurement during a test, at least one

acquired value consisted of at least 2 values for each FOBG sensor. The data processing was handled using MS Excel software. Figure 5 shows the FBGuard measuring device.

3 RESULTS AND DISCUSSION

The accuracy of the measurements taken from the FOBGs as well as their correlation with the failure sequence in the panels is crucial, as they will determine the effectiveness of the proposed SHM system. Interpretation of data is focused on the discussion of the comparability of the results gained from the FOBG and the applied resistance strain gauges with respect to minimising the local effects by installation of sensors at several locations.

Figure 6 shows the overview of the strain signals measured by both optical and resistance strain sensors during the static loading up to 70% of the expected Panel_1 failure load (solid lines correspond to strain gauges, and dashed lines correspond to optical sensors). Three different buckling modes in the skin bays occurred in panel_1 (at 60 kN, 160 kN and 250 kN). Figure 7 – Figure 9 show the comparison of the corresponding FOBG and SG strain signals of the sensors situated in the same areas in the panels. The data in Figure 7 represents sensors bonded onto the surface of Panel_1. The positions of the stringer sensors in Panel_1 are not located on the same stringers, but on different stringers in the same location. The sensors bonded on the stringers produced linear strain vs. force curves (left diagram) up to 92% of failure load. The loss of the foot stringer stability in the area of future failure is indicated by the nonlinearity of the signals in the final phase of loading. All of the sensors (FOBG and SG – right diagram) bonded to the skin surface are able to detect the development of the buckling waves. The same colours of the curves indicate the same skin locations of the sensors (FOBG sensors are placed into the inner side of the skin, and SG sensors are placed into the outer side of the skin). The large variation in the measurements indicates the large variation in the deformation of the areas around the locations of the sensors.

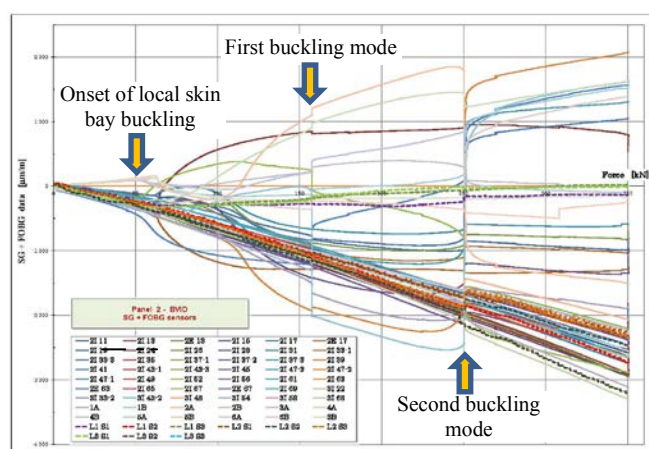


Figure 6: Comparison of FOBG (dash lines) and SG data vs. force (Panel_1)

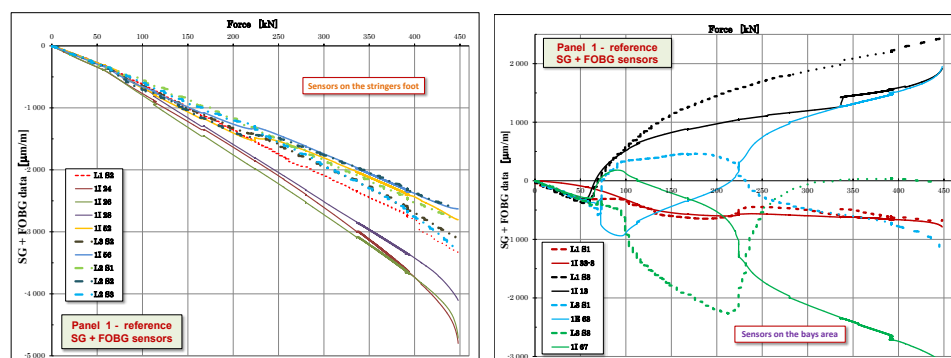


Figure 7: Comparison of FOBG (dash lines) and SG data vs. force– reference Panel_1

Figure 8 and Figure 9 show the comparison of the corresponding bonded SGs and the embedded FOBG sensors into the structure for each individual FOBG line of Panel_2 and Panel_3, respectively (see above mentioned sensors topology description). The locations of the SGs were selected so as to have some of the locations of the SGs to coincide with the locations of the FOBGs. The same colour of the curves indicates the same locations of the sensors. The FOBG sensors data are represented by dashed lines, and the corresponding data measured using SGs are displayed by solid and dot-dash lines.

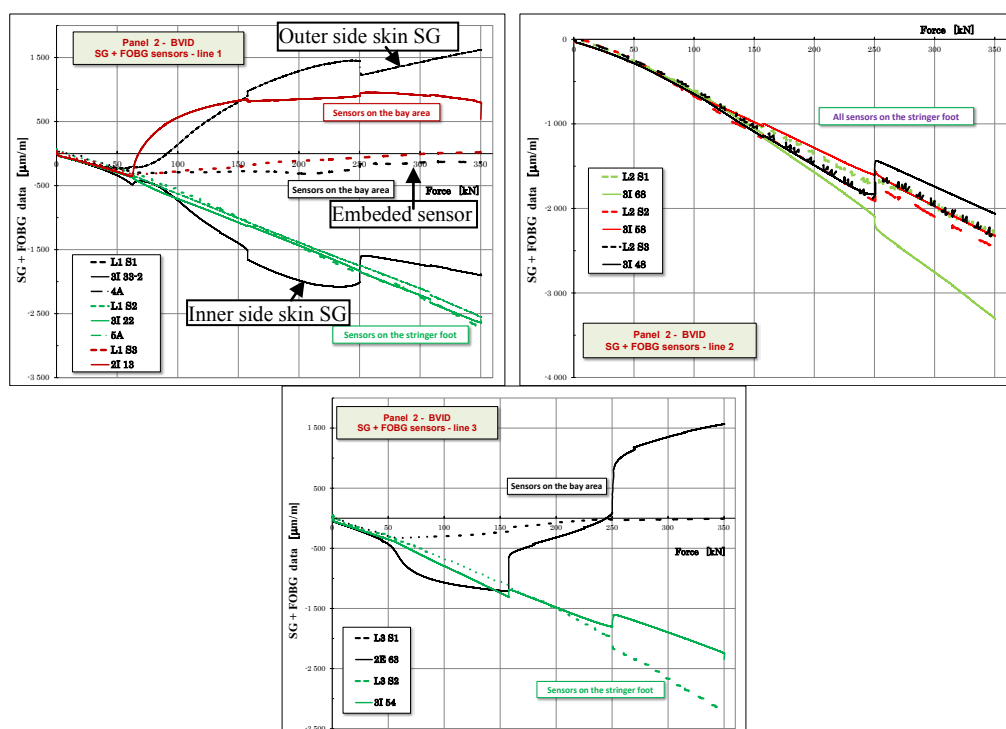


Figure 8: Comparison of FOBG (dash lines) and SG data vs. force – BVID Panel_2

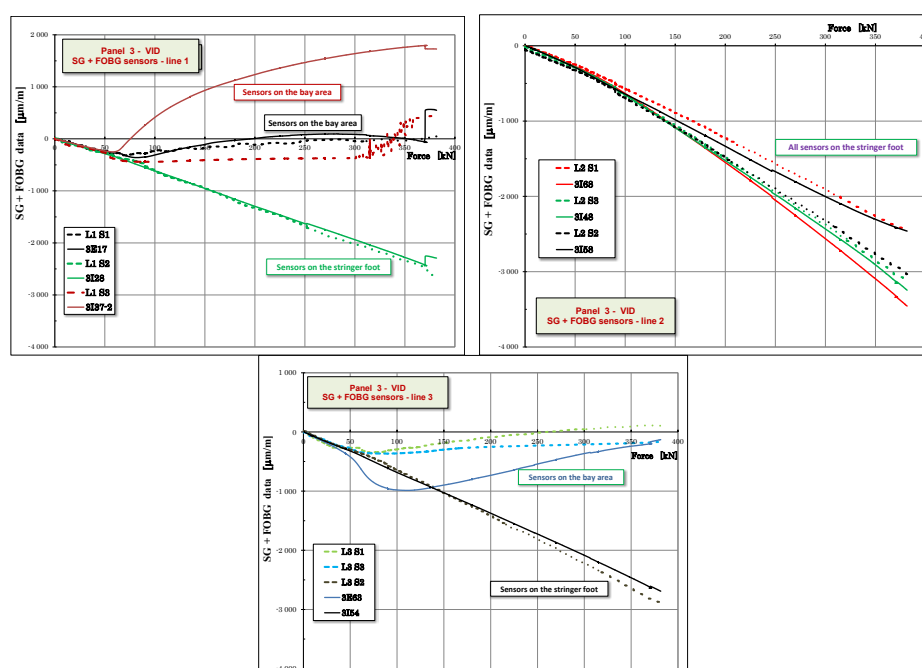


Figure 9: Comparison of FOBG (dash lines) and SG data vs. force – VID Panel_3

The L3S3 sensor in Panel_2 exhibited a small non-measurable peak. The fault of this sensor was most likely caused during manufacturing or the BVID creation process. The strain history of the L1S3 sensor in Panel_3 is not continuous – see Figure 10. The discontinuity in the range between 6.9 kN and 24.3 kN and the step at 54.2 kN cannot be explained by sudden deformation changes. The discontinuity was repeatedly measured, although no relevant deformations of the structure were registered. This discontinuity in the response can be considered as a rough sensor error due to the optical fibre or panel manufacturing. The rough data error can be eliminated by a constant scale (720 $\mu\text{m/m}$) subtraction, as shown in Figure 10. The low robustness of fibre optic sensors against damage and difficulties with fibre handling are important application problems.

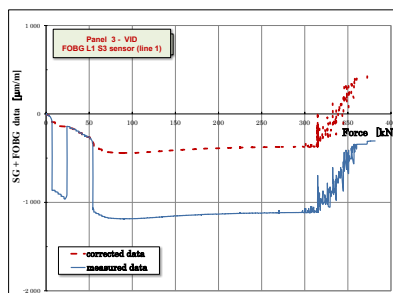


Figure 10: Modification of the FOBG data for the L1 S3 sensor – VID Panel_3

A perfect agreement between the FOBG and SG sensors is achieved for loads below the onset of local skin bay buckling for all the panels. At 65 kN, local buckling initiates at the bay where strain is measured. The measurements from the FOBG sensors and the SG sensors located into the foot of the stringers are quite close up to 250 kN for Panel_2. Subsequently, the buckling significantly influences the stinger foot area. After that point, the FOBG and SG data deviate significantly due to the alteration of the buckling modes, which results in the locations of the one type of sensor at positions of opposite curvature to those of the other type of sensor. Good agreement between the FOBG and SG sensors located in the stringer foot area up to failure for Panel_3 was achieved. The development of buckling waves was different in each of the tested panels.

Different situations in strain measurement occur for sensors placed into/onto the bays. The measured signals differ significantly after the onset of local skin bay buckling. The sensors placed on the skin provide good information about the maximum local deformations compared to the FOBG sensors embedded into the composite structure. The embedded sensors are not able to provide correct information about the local deformations. The embedded sensors are located near the neutral axis. The initiation of additional bending and local strength capacity loss as a consequence of the buckling onset implies that the local deformation on the surfaces and inside of the structure differ, as documented in Figure 8. Two strain gauges (3I 33-2, A4) and the L1S1 FOBG sensor are located in the same area of the bay – the SGs are bonded to the outer side and inner side of the skin, and the FOBG sensor is embedded into the skin. Both SGs indicate local flexural buckling and tension/compression conditions on the skin surfaces. This appearance implies that the embedded sensor must provide a low strain value in compliance with the measured data.

Equally important for the efficiency of the SHM concept is the capability of the FOBGs to capture the deformation events and the accuracy of the measured strain histories. In general, the FOBGs bonded onto the skin surface captured all the events in Panel_1 that are related to the change in the buckling mode of the skin. Thus, by having a priori a function between the local strains and the buckling behaviour of the panel (possibly derived from a numerical analysis), the measurements from the FOBGs can be translated into useful information regarding the structural health of the panel.

In all cases, prior to buckling, the measured strains between the sensors coincided. When buckling was initiated, the measurements of some of the sensors started to deviate, primarily due to the different buckling curvature of the measurement locations. The differences between the data were mainly observed in the case of the sensors that are placed on the skin in areas where buckling

curvature is significant. A non-linear strain vs. force curve is typical for the sensors located on the surface of the skin bays after the onset of the local buckling of the skin. On the contrary, the FOBG sensors embedded into the structure provide limited information on the buckling mode changes. Only the onset of buckling can be indicated. The subsequent development of the buckling waves and their changes are not indicated generally. This lack of sensitivity to these responses can be caused by the fact that the embedded FOBG sensors are placed into the structure very close to the neutral axis. Due to buckling, an additional bending originates in the structure. Both of these situations can result in the lack of sensitivity to the local buckling of the embedded sensors. Regarding final failure, the FOBG measurements did not provide a clear warning, possibly because final failure occurs suddenly. However, again, if the strain to failure is known, then the strain values of the FOBGs placed onto/into the stringers can be the warning themselves and can also provide information about the residual strength of the panel.

CONCLUSION

The comparison between strain measurements using FOBG sensors and SGs bonded onto/into composite panels was documented. The FOBG data and the SG data were found to be in good agreement if no buckling occurs. The differences between the measured signals of the optical sensors and those of the SGs during buckling were caused by two main factors: 1) the relative positions of the FOBG sensors and the SG sensors on a panel and 2) the positions of sensors on/into the laminate. The buckling waves and failure development were very well indicated during loading by all sensors located on the panel surface. The significant buckling amplitude caused bending, which can result in tension strain on one skin surface and compression strain on the opposite skin surface. In contrast, the embedded sensors within the skin suffered from low signals because of the lack of strain at the neutral axis. Good agreement between the data from the SGs and FOBG sensors was also achieved for all sensors placed on the stringers, which did not buckle. The good reliability of FOBG sensors during the fatigue and static testing up to failure of panels was verified, with the exception of one sensor, where a source of rough error was identified.

ACKNOWLEDGMENT

The research leading to these results has received funding from the European Community's Seventh Framework Programme (FP7/2007-2013) for the Clean Sky Joint Technology Initiative under grant agreement n° CSJU-GAM-GRA-2008-001 and grant agreement n° 296514.

REFERENCES

- [1] R. Jones, S. Galea. Health monitoring of composite repairs and joints using optical fibers. *Composite Structures*, 58(3):397–403 2002.
- [2] Y. Zhao, F. Ansari. Embedded fiber optic sensor for characterization of interface strains in FRP composite. *Sensors Actuators A: Phys.*, 100(2–3):247–51, 2002.
- [3] I. McKenzie, N. Karaffolas. Fiber Optic Sensing in Space Structures: The Experience of the European Space Agency. 17th International Conference on Optical Fibre Sensors. *Proceedings of SPIE Vol. 5855 SPIE, Bellingham, WA*, doi: 10.1117/12.623988, May 2005.
- [4] H. Tsutsui, A. Kawamata, T. Sanda, N. Takeda. Detection of impact damage of stiffened composite panels using embedded small-diameter optical fibers. *Smart Mater. Struct.* 13:1284–1290, 2004.
- [5] A. Papantoniou, G. Rigas, N.D. Alexopoulos. Assessment of the strain monitoring reliability of fiber Bragg grating sensor (FBGs) in advanced composite structures. *Comp. Structures*, 93:2163–2172, 2011.
- [6] S. Takeda, Y. Aoki, Y. Nagao. Damage monitoring of CFRP stiffened panels under compressive load using FBG sensors. *Comp. Structures*, 94:813–819, 2012.
- [7] FlexTest®40 control system manual, DS2.42684 311 Dynamic High Force System, *MTS System*, 2011.
- [8] BMCM module system user manual for PCI-Base (PCI-Base500/300, MAD/MDA, MVLxx), 2010.
- [9] NextView®4 User Manual Version 4.5, *BMC Messysteme GmbH*, 2011.
- [10] Demuth, J. User and Configuration Guide for the FBGuard 1550, Version 1.00, *Safibra s.r.o.*, 2012.